

Some exact solutions to the Lighthill Whitham Richards Payne traffic flow equations

G Rowlands¹, E Infeld² and A A Skorupski²

¹ Department of Physics, University of Warwick, Coventry CV4 7AL

² National Centre for Nuclear Research, Hoża 69, 00-681 Warsaw, Poland

E-mail: g.rowlands@warwick.ac.uk, einfeld@fuw.edu.pl, askor@fuw.edu.pl

Abstract. We find a class of exact solutions to the Lighthill Whitham Richards Payne (LWRP) traffic flow equations. Using two consecutive lagrangian transformations, a linearization is achieved. Next, depending on the initial density, we either apply (again two) Lambert functions and obtain exact formulas for the dependence of the car density and velocity on x, t , or else, failing that, the same result in a parametric representation. The calculation always involves two possible factorizations of a consistency condition. Both must be considered. In physical terms, the lineup usually separates into two offshoots at different velocities. Each velocity soon becomes uniform. This outcome in many ways resembles the two soliton solution to the Korteweg–de Vries equation. We check general conservation requirements. Although traffic flow research has developed tremendously since LWRP, this calculation, being exact, may open the door to solving similar problems, such as gas dynamics or water flow in rivers. With this possibility in mind, we outline the procedure in some detail at the end.

PACS numbers: 05.46.-a, 47.60.-l, 47.80.Jk

Submitted to: *J. Phys. A: Math. Gen.*

1. General history. Formulation of the model

We have found over the years that several nonlinear, partial differential equations of physics, not integrable by standard methods, such as Inverse Scattering or else an inversion of variables, yield their secrets to lagrangian coordinate methods [1]–[4]. Here we will treat one such equation pair and see a combination of two ‘lagrangian’ transformations (the second one will be called quasi-lagrangian for reasons to be explained) and a twofold introduction of the Lambert function enable us to solve the one lane traffic flow problem explicitly. A further class of solutions is found in parametric form.

Although we find a class of solutions that falls short of being general, common sense situations are well described, as well as some unexpected ones. The interesting thing, however, is that the much researched nonlinear equations involved, known for a long

time now, can in some instances be solved exactly, without recourse to approximations and with little or no numerics.

In 1955, James Lighthill and his former research student, Whitham, formulated an equation describing single lane traffic flow, assumed congested enough to justify a fluid model. The theory was formulated in the second part of their classic paper on kinematic waves [5]. Richards independently came to the same conclusion and published in the following year [6]. Next Payne [7] and Whitham [8] added a second equation and replaced the LWR equation with standard continuity. We will call this pair LWRP. Recently the literature on both models has grown considerably, see for example the books by Kern [9] and further references [10]–[18].

Extensions to more than one lane, lane changing, discrete models, higher order effects, as well as numerical work, prevail. One of the original authors has found a Toda lattice like solution to the discrete version of Newell [19], see [20]. In a future paper, we will see if the methods introduced here can be applied to some of these recent extensions of LWRP and LWR.

1.1. The model

Assume a long segment of a one lane road, deprived of entries and exits, sufficiently congested by traffic and free of breakdowns to admit a continuous treatment, so as to permit us to postulate the usual equation of continuity:

$$\frac{\partial \rho}{\partial t} + u \frac{\partial \rho}{\partial x} = -\rho \frac{\partial u}{\partial x}. \quad (1)$$

Here ρ is the density of cars, the maximum of which corresponds to a rather deplorable, but all too familiar almost bumper to bumper situation, and u is the local velocity. The right hand side of the second, newtonian equation, formulated by Payne [7] and Whitham [8], is less obvious:

$$\frac{\partial u}{\partial t} + u \frac{\partial u}{\partial x} = \frac{V(\rho) - u}{\tau_0} - \frac{\nu_0}{\rho} \frac{\partial \rho}{\partial x}. \quad (2)$$

The first term on the right involves the mean drivers' reaction time τ_0 , and the next term models a diffusion effect depending on the drivers' awareness of conditions beyond the preceding car. The constant ν_0 is a sort of diffusion coefficient, measuring the effect of the density gradient. Some recent improved models also bring in the second derivative, but we will not at this stage.

In particular, $u = V(\rho)$ and ρ both constant give a possible solution to the LWRP equations. Indeed, in his book Whitham expands around this equilibrium and treats the linear waves and possible instability so obtained [8]. However, exact nonlinear solutions are what we are interested in at the present.

We specify

$$V(\rho) = V_0 - h_0 \tau_0 \sqrt{\nu_0} \rho, \quad V_0 = \text{const.} \quad (3)$$

This often postulated form of $V(\rho)$ is the only one that leads to an integrable equation, as far as we can see. Fortunately, the plot of $Q(\rho) = \rho V(\rho)$, which people measure, is always convex and parabola-like, see Whitham's figure 3.1. Thus, so far luck is with us.

We introduce dimensionless variables by replacing

$$t \rightarrow t \tau_0, \quad (u, V_0) \rightarrow (u, V_0) \sqrt{\nu_0}, \quad x \rightarrow x \sqrt{\nu_0} \tau_0, \quad \rho \rightarrow \rho (h_0 \tau_0)^{-1}. \quad (4)$$

This leaves the continuity equation unchanged, and the newtonian equation takes the form:

$$\frac{\partial u}{\partial t} + u \frac{\partial u}{\partial x} = V_0 - \rho - u - \frac{1}{\rho} \frac{\partial \rho}{\partial x}. \quad (5)$$

2. Introducing lagrangian coordinates

The non-linearity on the left hand side of equations (1) and (5) can be eliminated by introducing lagrangian coordinates: $\xi(x, t)$, the initial position (at $t = 0$) of a fluid element which at time t was at x , and time t . In this description, the independent variable x becomes a function of ξ and t , as are the fluid parameters $\rho(\xi, t) = \rho(x(\xi, t), t)$ and $u(\xi, t) = u(x(\xi, t), t)$.

Here and in what follows we adopt the convention that a superposition of two functions which introduces a new variable is denoted by the same symbol as the original function, but of the new variable. Denoting by f either ρ or u , the basic transformation between eulerian coordinates x, t and lagrangian ones ξ, t can be written as

$$x(\xi, t) = \xi + \int_0^t u(\xi, t') dt', \quad \frac{\partial x}{\partial t} = u(\xi, t), \quad \frac{\partial f(\xi, t)}{\partial t} = \frac{\partial f(x, t)}{\partial t} + u \frac{\partial f(x, t)}{\partial x}. \quad (6)$$

We denote by $s(\xi)$ the number of cars between the last one at $\xi = \xi_{\min}$ and that at ξ :

$$s(\xi) = \int_{\xi_{\min}}^{\xi} \rho_0(\xi') d\xi', \quad \rho_0(\xi) = \rho(x = \xi, t = 0) \quad (7)$$

where $\rho_0(\xi)$ is the initial mass density distribution.

Here and in what follows, the subscript 0 always refers to $t = 0$. We will also use the superscript 0 to refer to $\xi = 0$.

There are no gaps in the line of traffic considered and therefore $\rho_0(\xi)$ is positive. Hence $s(\xi)$ is an increasing function starting at $s(\xi_{\min}) = 0$, and one can introduce a uniquely defined inverse function $\xi(s)$. The initial position of a fluid element can be specified by either ξ or s .

If a small initial interval $d\xi$ at $t = 0$ becomes dx at time t , mass conservation requires:

$$ds = \rho_0(\xi) d\xi = \rho(x, t) dx. \quad (8)$$

This leads to a mass conservation equation in lagrangian variables:

$$\frac{\partial x(s, t)}{\partial s} = \frac{1}{\rho(s, t)}, \quad (9)$$

and to a useful operator identity

$$\frac{1}{\rho(x, t)} \frac{\partial}{\partial x} = \frac{1}{\rho_0(\xi)} \frac{\partial}{\partial \xi} = \frac{\partial}{\partial s}. \quad (10)$$

Integrating (9) over s' from $s(\xi = 0)$ to s , we obtain the continuity equation in integral form:

$$X(s, t) \equiv x(s, t) - x(s^0, t) = \int_{s^0}^s \frac{ds'}{\rho(s', t)}, \quad s^0 = s(\xi = 0). \quad (11)$$

This indicates that if we know the car density in lagrangian coordinates $\rho(s, t)$, we can determine the evolving shape of the line of traffic, where the distance X is measured from the $\xi = 0$ car.

The analog of the continuity equation (1) is obtained by differentiating (9) by t . Using the middle part of (6) we obtain

$$\frac{\partial \psi(s, t)}{\partial t} = \frac{\partial u}{\partial s}, \quad \psi = \frac{1}{\rho}, \quad (12)$$

The newtonian equation in lagrangian coordinates is obtained from (5) and (10):

$$\frac{\partial u(s, t)}{\partial t} + u = V_0 - \rho - \frac{\partial \rho}{\partial s}. \quad (13)$$

Equation (13) is linear and can be solved to express $u(s, t)$ in terms of ρ . Again, using the middle part of (6) we can also calculate $x(s, t)$:

$$u(s, t) = e^{-t} \left[\int_0^t N(s, t') e^{t'} dt' + u(s, 0) \right], \quad (14)$$

$$N(s, t) = V_0 - \left[\rho + \frac{\partial \rho}{\partial s} \right], \quad (15)$$

$$\begin{aligned} x(s, t) &= \xi(s) + \int_0^t u(s, t') dt' \\ &= \xi(s) + u(s, 0) - u(s, t) + \int_0^t N(s, t') dt', \end{aligned} \quad (16)$$

where the function $u(s, 0)$ will be determined later.

3. Finding the fluid density

Differentiating the newtonian equation (13) by s , and using continuity (12), we obtain one equation for ψ :

$$\frac{\partial^2 \psi}{\partial t^2} - \frac{\partial}{\partial s} \left(\frac{1}{\psi^2} \frac{\partial \psi}{\partial s} \right) + \frac{\partial \psi}{\partial t} + \frac{\partial}{\partial s} \frac{1}{\psi} = 0. \quad (17)$$

This equation can be factorized in two possible ways, I and II:

$$\text{I:} \quad \left(\frac{\partial}{\partial t} + \frac{\partial}{\partial s} \frac{1}{\psi} \right) \left(\frac{\partial \psi}{\partial t} - \frac{1}{\psi} \frac{\partial \psi}{\partial s} + 1 + \psi \right) = 0, \quad (18)$$

and

$$\text{II:} \quad \left(\frac{\partial}{\partial t} - \frac{\partial}{\partial s} \frac{1}{\psi} \right) \left(\frac{\partial \psi}{\partial t} + \frac{1}{\psi} \frac{\partial \psi}{\partial s} - 1 + \psi \right) = 0. \quad (19)$$

We will find that the second factor in (18) best yields solutions such that $X \geq 0$, whereas that in (19) rules $X < 0$, where X is always the distance from the car that started at $x = 0$. Different pairing would lead to trouble.

If we denote equation (17) as $O\psi = 0$ and the decompositions by I and II, the following symmetries hold:

$$O = O_1^I O_2^I = O_1^{II} O_2^{II}, \quad O_i^I(\psi) = (-1)^{i+1} O_i^{II}(-\psi), \quad i = 1, 2. \quad (20)$$

In what follows, we will find solutions for which the second factor in one of equations (18), (19) vanishes, leaving a more general treatment to a possible later paper. We follow motion from left to right. Factorization also means that we can only introduce the initial value of the density (or ψ). The initial velocity $u(s, t = 0)$ will then follow except for a universal constant. We will have more to say about this later on.

The non-linearities in (18) and (19) (second factors) can be eliminated if one transforms the variables s, t to η, t in a way similar to the lagrangian transformation (6), though without the usual physical interpretation:

$$s(\eta, t) = \eta \mp \int_0^t \frac{dt'}{\psi(\eta, t')}, \quad \frac{\partial s}{\partial t} = \mp \frac{1}{\psi(\eta, t)}, \quad \frac{\partial \psi(\eta, t)}{\partial t} = \frac{\partial \psi(s, t)}{\partial t} \mp \frac{1}{\psi} \frac{\partial \psi}{\partial s}. \quad (21)$$

Solving the resulting linear equation

$$\frac{\partial \psi(\eta, t)}{\partial t} = \mp 1 - \psi$$

we obtain, in view of the fact that s and η are identical at $t = 0$,

$$\psi(\eta, t) = \mp 1 + e^{-t}[\psi_0(\eta) \pm 1], \quad \psi_0(\eta) \equiv \psi(s = \eta, 0). \quad (22)$$

For this $\psi(\eta, t)$ we have

$$\int_0^t \frac{dt'}{\psi} = \mp \ln[e^t \psi(\eta, t) / \psi_0(\eta)], \quad (23)$$

and finally, back to $\rho = 1/\psi$ and using (21),

$$s = \eta + \ln(1 \mp \rho_0(\eta)A(t)), \quad \rho_0(\eta) = \rho_0(s = \eta), \quad A(t) = e^t - 1. \quad (24)$$

In this relation, defining s in terms of η and t , $\rho_0(\eta)$ is defined by (7) but is expressed in terms s , where one has to rename s to η . Exactly the same procedure applies to $\psi_0(\eta)$ given by (22).

Using (22), we can express ρ in terms of η and t :

$$\rho(\eta, t) = \frac{1}{\mp 1 + e^{-t}[1/\rho_0(\eta) \pm 1]}, \quad (25)$$

which tends to $\rho_0(s)$ as $t \rightarrow 0$.

We are now in a position to determine the function $u(s, 0)$ needed in equations (14) and (16). Differentiate (13) by s and then subtract both sides of (17) from the result to obtain

$$\left(\frac{\partial}{\partial t} + 1\right)\left(\frac{\partial \psi}{\partial t} - \frac{\partial u}{\partial s}\right) = 0. \quad (26)$$

Solved by

$$\frac{\partial \psi}{\partial t} - \frac{\partial u}{\partial s} = f(s)e^{-t}. \quad (27)$$

Therefore, if $f(s) = 0$, equation (12) will be valid for all time. All we require is

$$\left[\frac{\partial \psi}{\partial t} - \frac{\partial u}{\partial s} \right]_{t=0} = 0, \quad \text{i.e.} \quad \frac{\partial u(s, 0)}{\partial s} = \frac{\partial \psi_0}{\partial t}. \quad (28)$$

This result, along with either (18) or (19), leads to

$$\frac{\partial u(s, 0)}{\partial s} = \pm \frac{1}{\psi_0} \frac{\partial \psi_0}{\partial s} \mp 1 - \psi_0.$$

Integrating over s' from s^0 to s and transforming the result to ξ , we end up with

$$u(\xi, 0) = u_0 - \xi \mp \left[s(\xi) - s^0 + \ln \frac{\rho_0(\xi)}{a} \right] \quad s^0 = s(\xi = 0), \quad a = \rho_0(\xi = 0), \quad (29)$$

where $u_0 = u(\xi = 0, 0) \geq 0$ is arbitrary.

The last task is to determine $u(s, t)$, $x(s, t)$, and $X(s, t)$, given by (14), (16), and (11), in terms of η . Using (25), (24) and (15) we find the integrand N :

$$\begin{aligned} N(s, t) &= V_0 - \left[\rho + \frac{\partial \rho}{\partial s} \right] = V_0 - \left[\rho + \frac{\partial \rho / \partial \eta}{\partial s / \partial \eta} \right] \\ &= V_0 \pm 1 - \frac{\pm 1 + \rho_0(\eta) + \rho'_0(\eta)}{1 \mp [\rho_0(\eta) + \rho'_0(\eta)](e^t - 1)}, \end{aligned} \quad (30)$$

which tends to $V_0 \pm 1$ as $t \rightarrow \infty$. Here $\eta = \eta(s, t)$ must be found as a solution of the transcendental equation (24), and the integrals (14) and (16) must be calculated numerically. On the other hand, the integral (11) can be calculated analytically:

$$\begin{aligned} X(s, t) &\equiv x(s, t) - x(s^0, t) = \int_{\eta^0}^{\eta} \frac{\partial s' / \partial \eta'}{\rho(\eta', t)} d\eta' \\ &= e^{-t} \left\{ \xi(s = \eta) - \xi(s = \eta^0) \mp A(t) \left[\eta - \eta^0 + \ln \frac{\rho_0(\eta)}{\rho_0(\eta^0)} \right] \right\}, \end{aligned} \quad (31)$$

where $\eta = \eta(s, t)$ and $\eta^0 = \eta(s^0, t)$ are defined implicitly by (24).

Notice that the time evolution of an assumed initial density profile $\rho_0(\xi)$ can only be determined if the solution $\eta(s, t)$ of equation (24) is a continuous function of t . This will be true either in case I, if $\rho_0(\xi)$ decreases from its initial value $a = \rho_0(\xi = 0)$ as ξ increases (i.e., for $\xi \geq 0$), or in case II, if $\rho_0(\xi)$ grows as ξ increases from $-\infty$ to 0.

In either case, $\eta(s, t)$ starts its time evolution with $\eta(s, 0) = s$. Then in case I, it grows to $\eta_{\max}(s) = \eta(s, t \rightarrow \infty)$, and in case II, it falls to $\eta_{\min}(s) = \eta(s, t \rightarrow \infty)$.

If $\rho_0(\xi)$ has a maximum at $\xi = \xi_m$ either for $\xi > 0$ or $\xi < 0$, then for any ξ within the interval $(0, \xi_m)$, $\eta(s(\xi), t)$ as a function of t would have a jump, which is unacceptable.

Another obvious requirement on the initial density profile $\rho_0(\xi)$ is its integrability over the interval $(-\infty, 0)$ or $(0, \infty)$.

In practice, the general theory given in the last two sections is only useful if the integral (7) can be determined analytically. Examples will be given in the following sections.

4. Two exponential profiles of the initial fluid density

We will see that two exponential profiles of the initial fluid density

$$\rho_0(\xi) = a \exp(-\lambda\xi), \quad \xi \geq 0, \quad \text{i.e.} \quad \xi_{\min} = 0, \quad (32)$$

$$\rho_0(\xi) = a \exp(\lambda\xi), \quad \xi \leq 0, \quad \text{i.e.} \quad \xi_{\min} = -\infty, \quad (33)$$

play a special role here, as in their case it is possible to eliminate the auxiliary variable η , and even find the fluid density ρ in terms of X and t . This is because the argument of the logarithm in equation (24) defining $\eta(s, t)$ is a linear function of η . Therefore the solution $\eta(s, t)$ of (24) can be given in terms of the Lambert function $W(x)$ defined by

$$W \exp(W) = x, \quad \text{equivalent to} \quad W + \ln W = \ln x, \quad -1/e \leq x < \infty. \quad (34)$$

The W function is named after Johann Heinrich Lambert, Leonhard Euler's young protégé and an important mathematician in his own right (1728–1777), see [21] for a summary. For negative x , W has two negative branches and the upper one (continuous at $x = 0$) along with the main branch of the logarithms should be chosen in what follows ($\ln x = \ln |x| + i\pi$ when $x < 0$).

The solution Y of the transcendental equation

$$Y + \ln(aY + b) = c \quad (35)$$

is given by

$$Y = W \left[\exp \left(c + \frac{b}{a} - \ln a \right) \right] - \frac{b}{a}. \quad (36)$$

Using equation (7) we first find

$$s^0 = s(\xi = 0) = \int_{\xi_{\min}}^0 \rho_0(\xi') d\xi' = \begin{cases} 0 & \text{for (32),} \\ \frac{a}{\lambda} & \text{for (33),} \end{cases} \quad (37)$$

and then calculate

$$\begin{aligned} s(\xi) &= s^0 + \int_0^\xi \rho_0(\xi') d\xi' = s^0 \mp \frac{a}{\lambda} (\exp(\mp \lambda\xi) - 1) \\ &= \begin{cases} \frac{a}{\lambda} (1 - \exp(-\lambda\xi)) & \text{for (32),} \\ \frac{a}{\lambda} \exp(\lambda\xi) & \text{for (33).} \end{cases} \end{aligned} \quad (38)$$

The inverse functions are given by

$$\xi(s) = \mp \frac{1}{\lambda} \ln \left(1 \mp \frac{\lambda}{a} (s - s^0) \right) = \begin{cases} -\frac{1}{\lambda} \ln \left(1 - \frac{\lambda s}{a} \right) & \text{for (32),} \\ \frac{1}{\lambda} \ln \frac{\lambda s}{a} & \text{for (33).} \end{cases} \quad (39)$$

Using this formula we can transform the initial conditions (32) and (33) given above in x, t to s, t :

$$\rho_0(s) = a \mp \lambda(s - s^0) = \begin{cases} a - \lambda s & \text{for (32),} \\ \lambda s & \text{for (33).} \end{cases} \quad (40)$$

We now look for solutions to equations (18) and (19) that recreate the above initial conditions as t tends to zero.

Replacing s by η in (40) and using the $\rho_0(\eta)$ so obtained in (24), we can write the result as

$$s = \eta + \ln \left\{ \lambda A(t) \eta + \left[1 + A(t)(\mp a - \lambda s^0) \right] \right\}. \quad (41)$$

Indeed the argument of the logarithm is a linear function of η , and we can use equations (35) and (36) to obtain

$$\begin{aligned} \eta(s, t) &= w(s, t) \pm \frac{a}{\lambda} + s^0 - \frac{1}{\lambda A(t)}, \quad A(t) = e^t - 1, \\ w(s, t) &= W \left\{ \exp \left[p(s, t) \right] \right\}, \\ p(s, t) &= s - s^0 \mp \frac{a}{\lambda} + \frac{1}{\lambda A(t)} + \ln \frac{1}{\lambda A(t)}. \end{aligned} \quad (42)$$

Inserting this $\eta(s, t)$ into (25) we obtain, in view of (40)

$$\rho(s, t) = \pm \frac{e^t}{A(t)} \left[\frac{1}{\lambda A(t) w(s, t)} - 1 \right]. \quad (43)$$

We recover the initial condition (40) when $t \rightarrow 0^+$, and so $1/A(t) \rightarrow \infty$, by invoking the large argument approximation for W : $W(x) \approx \ln(x) - \ln \ln(x)$, $x \gg 1$,

$$\begin{aligned} \rho &\rightarrow \pm \frac{1}{A} \left[\frac{1}{\lambda A(s - s^0 \mp \frac{a}{\lambda} + \frac{1}{\lambda A})} - 1 \right] = \frac{a \mp \lambda(s - s^0)}{1 + A(\lambda(s - s^0) \mp a)} \\ &= a \mp \lambda(s - s^0) + O(A). \end{aligned} \quad (44)$$

Using (43) and (29) we can determine $N(\xi, t)$ and $u(\xi, 0)$ needed in equations (14)–(16), where $s = s(\xi)$ is given by (38):

$$\begin{aligned} N(\xi, t) &= V_0 \pm 1 \pm \frac{e^{-t}}{1 - e^{-t}} \left[1 - \frac{1}{\lambda(1 - e^{-t})(1 + w(s, t))} \right] \\ &\rightarrow V_0 \pm 1 \quad \text{as } t \rightarrow \infty, \end{aligned} \quad (45)$$

$$u(\xi, 0) = u_0 + (\lambda - 1)\xi + \frac{a}{\lambda} \left[\exp(\mp \lambda \xi) - 1 \right], \quad (46)$$

where in equation (45) we used the fact that for large t , $w(s, t) \approx -\ln[\lambda(e^t - 1)]$ which tends to minus infinity as $t \rightarrow \infty$. Calculating the integrals in (14) and (16) numerically, we can find characteristics $x(\xi, t)$ parametrized by the initial fluid element position ξ , shown in figures 2 and 4.

We will now try to express ρ directly in terms of X by using (11). Inserting $\rho(s, t)$ given by (43) into (11) and changing the integration variable from s to w we obtain

$$\begin{aligned} -\lambda X &= \pm \lambda^2 A^2(t) e^{-t} \int_{s^0}^s ds' \frac{w(s', t)}{\lambda A(t) w(s', t) - 1} \\ &= \pm \lambda A(t) e^{-t} \int_{w(s^0, t)}^{w(s, t)} dw' \left[1 + \frac{1 + \lambda A(t)}{\lambda A(t) w' - 1} \right] \\ &= \pm e^{-t} \left\{ \lambda A(t) [w(s, t) - w(s^0, t)] \right. \\ &\quad \left. + [1 + \lambda A(t)] \ln \frac{\lambda A(t) w(s, t) - 1}{\lambda A(t) w(s^0, t) - 1} \right\}, \end{aligned} \quad (47)$$

which can be written as

$$Y + \ln\left([1 + \lambda A(t)]Y - 1\right) = \frac{\mp \lambda e^t X + \lambda A(t)w(s^0, t)}{1 + \lambda A(t)} + \ln(\lambda A(t)w(s^0, t) - 1),$$

where

$$Y = \frac{\lambda A(t)w(s, t)}{1 + \lambda A(t)}.$$

Again using (35) and (36) to solve for Y , we find $\lambda A(t)w(s, t)$ as a function of X and t . Inserting it into (43) we end up with

$$\rho(X, t) = \begin{cases} \mp \frac{[1 + \lambda A(t)]W(e^\phi)}{(1 - e^{-t})\{1 + [1 + \lambda A(t)]W(e^\phi)\}}, & X \geq 0, \\ 0, & X < 0, \end{cases} \quad (48)$$

where

$$\phi = \frac{\mp \lambda e^t X + \lambda A(t)w(s^0, t) - 1}{1 + \lambda A(t)} + \ln \frac{\lambda A(t)w(s^0, t) - 1}{1 + \lambda A(t)}. \quad (49)$$

Note that equation (47) could also be obtained from (31), where η is given by (42),

$$\lambda[\xi(s = \eta) - \xi(s = \eta^0)] = \mp \ln \frac{a \mp \lambda(\eta - s^0)}{a \mp \lambda(\eta^0 - s^0)}$$

in view of (39), and ρ_0 is given by (40) with $s = \eta$.

As $t \rightarrow 0$ we recover the initial condition (32) or (33) by once again invoking the large argument approximation $W(x) \approx \ln(x) - \ln \ln(x)$. The calculation is similar to that in s, t above.

4.1. Exponentially decreasing initial fluid density

As initial condition at $t = 0$ we first take a pulse described by (32) and subsequently expected to move to the right. To the far right cars are thin on the ground. We expect them to move freely and make it possible for the congestion near the discontinuity to spread out. This common sense expectation will test our result.

The density profile $\rho(X, t)$, defined by equation (48) with upper sign is shown in figure 1.

As $t \rightarrow \infty$ this profile tends to

$$\rho \rightarrow \begin{cases} \frac{[1 - \exp(-a/\lambda)] \exp(-X)}{1 - [1 - \exp(-a/\lambda)] \exp(-X)}, & X \geq 0, \\ 0, & X < 0. \end{cases} \quad (50)$$

That is because $AW \approx -[1 - \exp(-a/\lambda)] \exp(-X)$, as small argument W functions can be approximated by their argument, $W(x) \approx x$, regardless of sign. The initial condition only appears as the ratio a/λ . A whole class of initial profiles ends up developing identically, as long as this ratio is the same (figure 1).

In figure 2 we present characteristics $x(\xi, t)$ obtained by numerically calculating the integrals in (14) and (16). No crossing of characteristic curves is observed, a pleasing

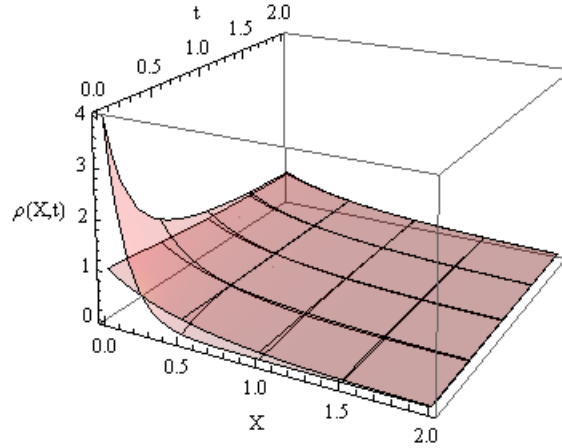


Figure 1. Two density profiles for various times as found from our solution (I). Here $a = 1$, $\lambda = 2$ in the first case, and $a = 4$, $\lambda = 8$ in the second one. Nevertheless, the emerging profiles are seen to be identical after a while. The value of a for each surface can be seen as equal to $\rho(0, 0)$.

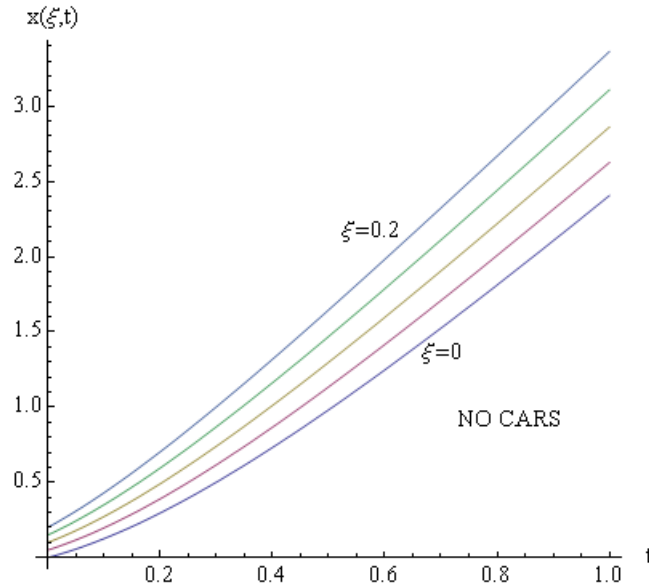


Figure 2. Characteristics $x(\xi, t)$ as functions of t for ξ ranging from 0 to 0.2 in steps of 0.05, $a = 4$, $\lambda = 8$, $u_0 = 1$, and $V_0 = 2$.

vindication of the LWPR model. In particular, the $\xi = 0$ line in figure 2 gives us the trajectory of the discontinuity point, defining X .

Equation (45) with upper sign implies a uniform motion at the final, large t stage, at which $u = V_0 + 1$. This can also be seen from equation (2). This emerging solution is identical to that given by Whitham [8] as a special case of a ‘continuous shock structure’, Whitham’s equation (3.16), (when his $A = 0$, $U - v = 0$). Of course, continuity is lost at $s = 0$. Now we know exactly how to set up initial conditions so as to obtain this profile. Alternatively, we could set up this profile from the beginning. There are obviously

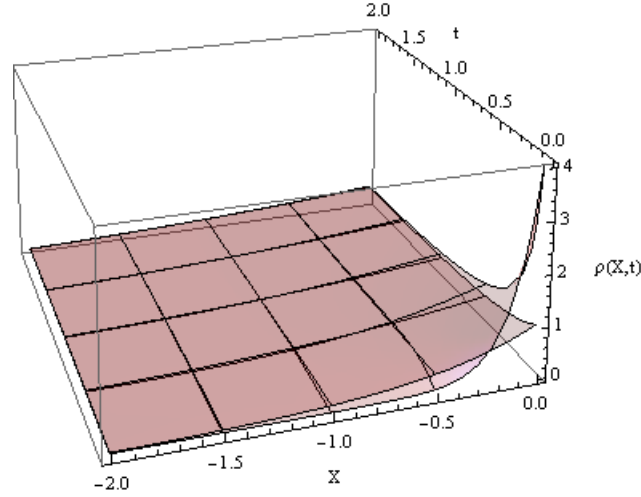


Figure 3. Two density profiles for various times as found from our solution (II). Here $a = 1$, $\lambda = 2$ in the first case, and $a = 4$, $\lambda = 8$ in the second one. Nevertheless, the emerging profiles are seen to be identical after a while. The value of a for each surface can be seen as equal to $\rho(0, 0)$. Notice that the final amplitude of ρ is smaller here than in figure 1.

fewer possible final states than initial conditions, a state of affairs often encountered in non-linear problems, see e.g. [22, 23], and [2] for further references.

We can now check to see if the integral of ρ is conserved in the $t \rightarrow \infty$ limit. In view of (50)

$$\rho(X, t \rightarrow \infty) = \frac{\partial}{\partial X} \ln \left\{ 1 - [1 - \exp(-a/\lambda)] \exp(-X) \right\},$$

which implies

$$\int_0^\infty \rho(X, t \rightarrow \infty) dX = a/\lambda.$$

The integral over all X of $\rho(X, t \rightarrow \infty)$ is indeed a/λ . Our exact solution converges to a stationary mass conserving travelling wave.

4.2. Exponentially increasing initial fluid density

We now find a similar solution, but to case II. Our initial condition (33) is now limited to $x \leq 0$.

This is the mirror image of the previous lineup, with the most congested traffic facing an empty road. However, motion will still be from left to right.

The density profile $\rho(X, t)$, defined by equation (48) with lower sign is shown in figure 3. As $t \rightarrow \infty$ this profile tends to

$$\rho \rightarrow \begin{cases} \frac{[\exp(a/\lambda) - 1] \exp(X)}{1 + [\exp(a/\lambda) - 1] \exp(X)}, & X \leq 0, \\ 0, & X > 0. \end{cases} \quad (51)$$

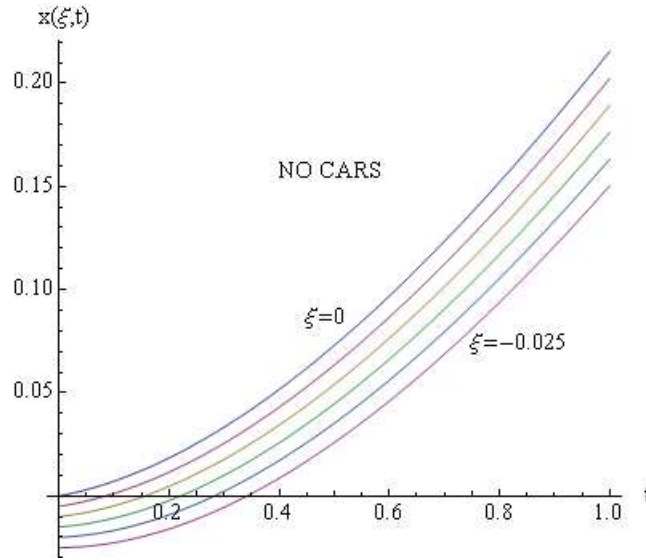


Figure 4. Characteristics $x(\xi, t)$ as functions of t for ξ ranging from 0 to -0.025 in steps of -0.005 , $a = 1$, $\lambda = 2$, $u_0 = 0.05$, and $V_0 = 10$.

The end result is very similar to the previous one, but not identical. Mass conservation follows from the same calculation. However, we are solving a different equation and the asymptotic, uniform velocity is $V_0 - 1$ as opposed to the $V_0 + 1$ of case I, see (45) with lower sign. This can also be seen from figure 4, where characteristics $x(\xi, t)$ are presented.

If we match the initial velocities at the centre, $x = 0$, then after a while, two cavalcades emerge, a faster one at velocity $u = V_0 + 1$, and a slower one at $V_0 - 1$ (cheaper cars?) see figure 4. Our situation reminds us of solutions to the wave equation. Here $(c \partial_x - \partial_t)\psi = 0$ would correspond to I, $(c \partial_x + \partial_t)\psi = 0$ to II. Coexistence of the two was not surprising in the linear world, now it is somewhat unexpected. Although we are combining two solutions following from different factorizations of the governing equation, we should remember that we are nevertheless dealing with one exact solution, unique to the initial profile and velocities.

5. The initial density profiles that can be treated parametrically

In this section we present a few initial density profiles satisfying the applicability conditions of our theory as formulated at the end of section 3, see figure 5.

Detailed calculations will be performed for a pair of cases:

$$\rho_0(\xi) = \frac{a}{\cosh^2(\lambda\xi)} \equiv a [1 - \tanh^2(\lambda\xi)], \quad (52)$$

where either $0 \leq \xi < \infty$ in case I, or $-\infty < \xi \leq 0$ in case II.

The fact that the derivative $d\rho_0(\xi)/d\xi$ vanishes at $\xi = 0$, in contrast to the exponential profiles (32) and (33), will have a consequence on the time evolution in case I, see figure 6.

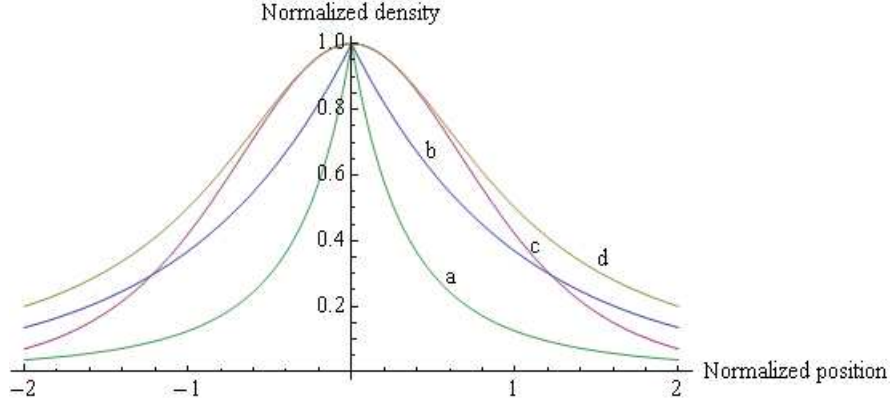


Figure 5. Normalized density profiles $\bar{\rho}_0 = \rho_0/a$ versus normalized position $\bar{\xi} = \lambda\xi$ for $\rho_0(\xi)$ given by (a): (32) and (33), (b): (54) for $b = 1$, $r = 3$, (c): (52), and (d): (53).

The remaining profiles will have a power behaviour at infinity, $\rho_0(\xi) \rightarrow (\pm\xi)^{-r}$ as $\pm\xi \rightarrow \infty$, where r is a real number greater than unity for integrability:

$$\rho_0(\xi) = \frac{a}{1 + (\lambda\xi)^2}, \quad (53)$$

and

$$\rho_0(\xi) = a \frac{b^r}{(\pm\lambda\xi + b)^r}, \quad b > 0, \quad r > 1, \quad (54)$$

where the upper sign refers to case I, $\xi \geq 0$, and the lower one to case II, $\xi \leq 0$.

By analogy to the exponential profiles (32) and (33), each pair of symmetric cases can be treated in a single calculation. For $\rho_0(\xi)$ given by (52) we first find

$$s^0 = s(\xi = 0) = \int_{\xi_{\min}}^0 \rho_0(\xi') d\xi' = \begin{cases} 0 & \text{for } \xi \geq 0, \\ \frac{a}{\lambda} & \text{for } \xi \leq 0, \end{cases} \quad (55)$$

and then calculate

$$s(\xi) = s^0 + \int_0^\xi \rho_0(\xi') d\xi' = s^0 + \frac{a}{\lambda} \tanh(\lambda\xi). \quad (56)$$

The inverse functions are given by

$$\xi(s) = \frac{1}{2\lambda} \ln \frac{1 + \lambda(s - s^0)/a}{1 - \lambda(s - s^0)/a} = \begin{cases} \frac{1}{2\lambda} \ln \frac{1 + \lambda s/a}{1 - \lambda s/a} & \text{for } \xi \geq 0, \\ \frac{1}{2\lambda} \ln \frac{\lambda s/a}{2 - \lambda s/a} & \text{for } \xi \leq 0. \end{cases} \quad (57)$$

Using $\tanh(\lambda\xi)$ calculated from (56) in (52) we obtain

$$\rho_0(s) = a \left[1 - \left(\lambda(s - s^0)/a \right)^2 \right] = \begin{cases} a[1 - (\lambda s/a)^2] & \text{for } \xi \geq 0, \\ \lambda s(2 - \lambda s/a) & \text{for } \xi \leq 0. \end{cases} \quad (58)$$

Replacing here s by η and using the $\rho_0(\eta)$ so obtained in (24) and (30) along with (56) we find equations defining $\eta(\xi, t)$ and the integrand $N(\eta, t)$ needed in equations (14)–(16):

$$\frac{a}{\lambda} \tanh(\lambda\xi) = \eta + \ln\left(1 - a[1 - (\lambda\eta/a)^2]A(t)\right), \quad \text{for } \xi \geq 0, \quad (59)$$

$$\frac{a}{\lambda}[1 + \tanh(\lambda\xi)] = \eta + \ln\left(1 + \lambda\eta(2 - \lambda\eta/a)A(t)\right), \quad \text{for } \xi \leq 0, \quad (60)$$

$$N(\eta, t) = V_0 \pm 1 + \frac{\mp 1 - f(\eta)}{1 \mp f(\eta)A(t)}, \quad (61)$$

where

$$f(\eta) = \begin{cases} -\eta(\eta + 2)\lambda^2/a & \text{for } \xi \geq 0, \\ \lambda[-\eta^2\lambda/a + 2\eta(1 - \lambda/a) + 2] & \text{for } \xi \leq 0. \end{cases} \quad (62)$$

In a similar way we can determine $X(\eta, t)$ by using (31) along with (57) and (58) with $s = \eta$:

$$X = -\frac{e^{-t}}{\lambda} \left[\left(\lambda A(t) + \frac{1}{2} \right) \ln \frac{1 - \lambda\eta/a}{1 - \lambda\eta^0/a} + \left(\lambda A(t) - \frac{1}{2} \right) \ln \frac{1 + \lambda\eta/a}{1 + \lambda\eta^0/a} + \lambda A(t)(\eta - \eta^0) \right] \quad \text{for } \xi \geq 0, \quad (63)$$

$$X = \frac{e^{-t}}{\lambda} \left[\left(\lambda A(t) + \frac{1}{2} \right) \ln \frac{\eta}{\eta^0} + \left(\lambda A(t) - \frac{1}{2} \right) \ln \frac{2 - \lambda\eta/a}{2 - \lambda\eta^0/a} + \lambda A(t)(\eta - \eta^0) \right] \quad \text{for } \xi \leq 0. \quad (64)$$

Using here $\eta(\xi, t)$ defined implicitly by either of equations (60) and in $\rho(\eta, t)$ given by (25), we obtain $\rho(X, t)$ in parametric form: $\rho(\xi, t)$ and $X(\xi, t)$. This form is appropriate for making use of the ParametricPlot3D command of *Mathematica*. The results are shown in figures 6 and 7. They resemble those shown in figures 1 and 2 except for the time evolution of the discontinuity at $X = 0$, $\rho(X = 0, t)$ for case I ($\xi \geq 0$), shown in figure 6.

The characteristics $x(\xi, t)$ can be found from equations (14)–(16) by numerical integration, where the integrand $N(\xi, t)$ is defined by (61) and either of equations (60), and

$$u(\xi, 0) = s_0 - \xi \mp \left\{ \frac{a}{\lambda} \tanh(\lambda\xi) - 2 \ln[\cosh(\lambda\xi)] \right\}, \quad (65)$$

see equations (29), (52) and (56). The results, depending on two parameters V_0 and u_0 , are shown in figure 8.

A characteristic feature of the plots representing the density given in parametric form, $\rho(\xi, t)$ and $X(\xi, t)$, is that the mesh lines correspond to $\xi = \text{const}$, and $t = \text{const}$, see figures 6 and 7. For the density given explicitly, $\rho(X, t)$, they correspond to $X = \text{const}$, and $t = \text{const}$, see figures 1 and 2. The mesh lines $\xi = \text{const}$ are particularly useful. Each point on a $\xi = \text{const}$ mesh line gives us the information of both the actual position X and the associated density at time t , for the car that started from $X = \xi$ at $t = 0$. This information is given in the frame moving along with the discontinuity at

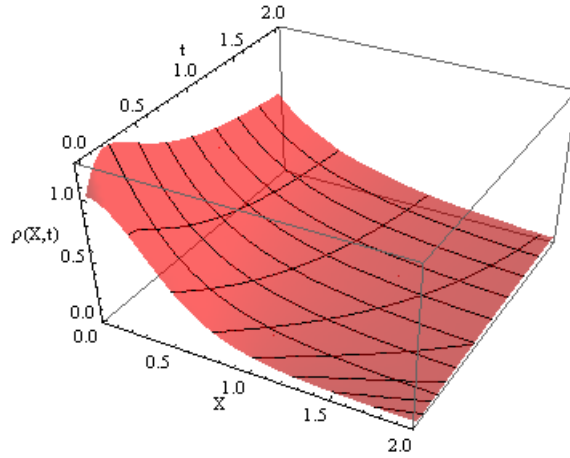


Figure 6. The fluid density represented parametrically as found from our solution (I). Here $a = 1$, $\lambda = 2$. The mesh lines correspond to $t = \text{const}$ or $\xi = 0, 0.25, 0.5, 0.75, \dots$. Each value of ξ is equal to X at $t = 0$.

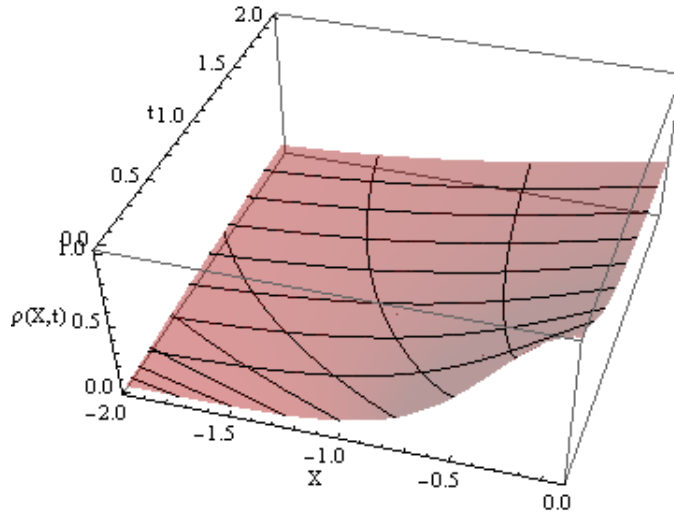


Figure 7. The fluid density as in figure 6 but as found from our solution (II). Here again $a = 1$, $\lambda = 2$, and $\xi = 0, -0.25, -0.5, -0.75, \dots$, see X at $t = 0$.

$\xi = 0$. The motion of these frames in turn is described by the characteristics labelled with $\xi = 0$ in figure 8.

Adding cases I and II, we have a solution such that the initial congestion splits in the middle, resulting once again in a slower cavalcade following a faster one, see figure 8. This is rather like a two soliton solution of the Korteweg–de Vries equation, see e.g. [2].

6. Summary

Our solutions augment those found for simpler, single equation nonlinear models, e.g. Burgers, see [8]. Our exact solutions converge to single or double stationary travelling

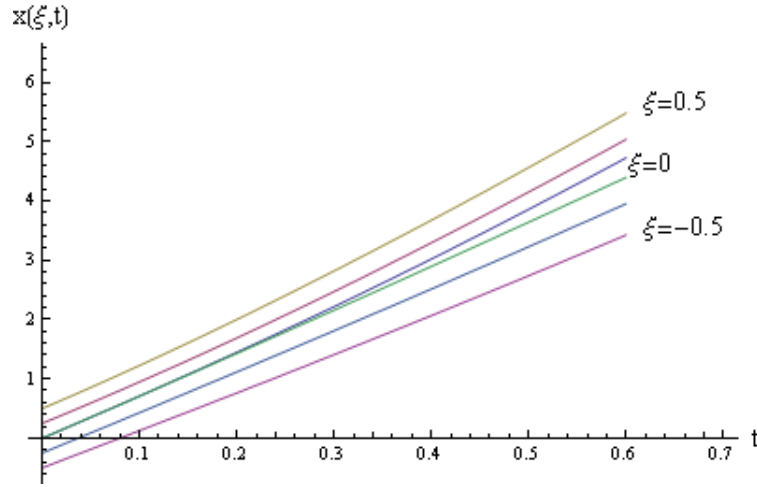


Figure 8. Characteristics $x(\xi, t)$ as functions of t for $\xi = 0, 0.25, 05$, and $\xi = 0, -0.25, -05$, $a = 1$, $\lambda = 2$, $u_0 = 7$, and $V_0 = 10$.

wave structures after a few τ_0 (figure 1). This steady state convergence is more or less what one would expect, at least in the single case. The LWRP equations have several families of solutions, to which we hereby add. Generally we must use common sense to home in on the relevant ones. However, exact solutions help and absolve us from the need to guess. As in police work, connecting initial conditions with a present situation requires painstakingly following through the history. Exact solutions exempt us of this task.

We introduce a lagrangian transformation in x, t . The variables are now ξ, t , ξ being the position at $t = 0$. It labels the car rather than its actual position. The continuity equation is now linear, simplifying further calculations. It may so happen that the newtonian equation can yield a condition in just one dependent variable. If this condition can be factorized, there is a possibility of finding exact solutions by finding solutions to this factorized equation, being of lower order. In our case, two distinct factorizations were possible, both were solved, and both solutions were needed to cover all x . In fact, each factorization was assigned to a specific half axis, the same for all cases considered. This situation, demanding merging two solutions to cover the whole domain, is unusual in a nonlinear problem. Another requirement was that the original profile have only one maximum at $x = 0$.

We had to introduce a second, quasi lagrangian transformation to linearise. In general, we obtain the solution in parametric form. However, if we are lucky, we can solve completely, that is get rid of the parameter, by using Lambert functions. We give an example of this.

It should be stressed that a complete solution is only possible if we combine our two factorized equations, I and II. This is similar to the situation for solutions to the wave equation

$$\left(c^2 \frac{\partial^2}{\partial x^2} - \frac{\partial^2}{\partial t^2}\right)\psi = 0$$

such that solutions of $(c\partial_x - \partial_t)\psi = 0$ and $(c\partial_x + \partial_t)\psi = 0$ coexist. However, this coexistence is somewhat surprising for a nonlinear system.

An interesting question is: how wide a class of non-linear problems can be so solved? Perhaps one possibility is furnished by the somewhat similar gas dynamics and shallow water equations? In our case, exponential initial conditions alone seem to promise that the Lambert function will make an appearance. Perhaps they should be used for similar problems.

Another interesting question is how general is the requirement of merging solutions I and II when two factorizations of the consistency condition exist.

Acknowledgments

We thank Drs M. Grundland and P. Goldstein for pointing out that our equations I and II are both integrable and non-Painlevé, a rare combination in mathematical physics.

References

- [1] Infeld E and Rowlands G 1989 Relativistic bursts *Phys. Rev. Lett.* **62** 1122–25
 Infeld E and Rowlands G 1997 Lagrangian picture of plasma physics I *J. Tech. Phys.* **38** 607–45
 Infeld E and Rowlands G 1998 Lagrangian picture of plasma physics II *J. Tech. Phys.* **39** 3–35
- [2] Infeld E and Rowlands G 2000 *Nonlinear Waves, Solitons and Chaos* 2nd edn (Cambridge: Cambridge University Press)
- [3] Infeld E, Rowlands G and Skorupski A A 2009 Analytically solvable model of nonlinear oscillations in a cold but viscous and resistive plasma *Phys. Rev. Lett.* **102** 145005 (doi: 10.1103/PhysRevLett.102.145005)
- [4] Skorupski A A and Infeld E 2010 Nonlinear electron oscillations in a viscous and resistive plasma *Phys. Rev. E* **81** 056406 (doi: 10.1103/PhysRevE.81.056406)
- [5] Lighthill M J and Whitham G B 1955 On kinematic waves, I Fluid movement in long rivers; II Theory of traffic flow on long crowded roads *Proc. R. Soc. A* **229** 281–345 (doi: 10.1098/rspa.1955.0088)
- [6] Richards P I 1956 Shock waves on the highway *Oper. Res.* **4** 42–51
- [7] Payne H J 1971 *Mathematical models of public systems in simulation Councils Proceedings* **1** 51–60
- [8] Whitham G B 1974 *Linear and Nonlinear Waves* chap 3 (New York: John Wiley)
- [9] Kern B S 2003 *The physics of traffic flow* (Berlin: Springer)
 Kern B S 2009 *Introduction to Modern Traffic Flow, Theory and Control* (Berlin: Springer)
- [10] Chandler R E, Herman R and Montroll E W 1958 Traffic dynamics: studies in car following *Oper. Res.* **6** 165–84
- [11] Greenberg H 1959 An analysis of traffic flow *Oper. Res.* **7** 79–85
- [12] Herman R, Montroll E W, Potts R B and Rothery R W 1959 Traffic dynamics: analysis of stability in car following *Oper. Res.* **7** 86–106
- [13] Jin W L and Zhang H M 2003 The formation and structure of vehicle clusters in the Payne–Whitham traffic flow model *Transportation Research* **37** 207–23
- [14] Kerner B S, Klenov L and Konhauser P 1997 Asymptotic theory of traffic flow *Phys. Rev. E* **56** 4200–16
- [15] Komentani E and Sasaki T 1958 On the stability of traffic flow *Oper. Res. Jpn.* **2** 11–26
- [16] Lua Y *et al* 2008 Explicit construction of solutions for the Lighthill–Whitham–Richards traffic flow model with a piecewise traffic flow density model *Transportation Research* **42** 355–72

- [17] Papageorgiou M 1983 *Application of Automatic Control Concepts in Traffic Flow and Control* (Berlin: Springer)
- [18] Zhang M, Shu C, Wong G C K and Wong S C 2003 A weighted essentially non-oscillatory numerical scheme for a multi-class LWR traffic flow model *J. Comp. Phys.* **191** 639–59
- [19] Newell G F 1961 Nonlinear effects in the dynamics of car following *Oper. Res.* **9** 209–29
- [20] Whitham G B 1990 Exact solutions for a discrete system arising in traffic flow *Proc. R. Soc. A* **428** 49–69 (doi:10.1098/rspa.1990.0025)
- [21] Corless R M, Gonnet G H, Hare D E G, Jeffrey D J and Knuth D E 1996 On the Lambert W function *Adv. in Comp. Math.* **5** 329–59
- [22] Armstrong T and Montgomery D 1967 Asymptotic state of the two-stream instability *J. Plasma Phys.* **1** 425–33 (doi: 10.1017/S0022377800003421)
- [23] Jordan P M and Puri P 2002 Exact solution for the unsteady plane Couette flow of a dipolar fluid *Proc. R. Soc. A* **458** 1245–72